Journal of Chemical and Petroleum engineering 2019, 53(1): 91-100
DOI: 10.22059/jchpe.2019.273826.1265

RESEARCH PAPER

Absolute Permeability Calculation by Direct Numerical Simulation in Porous Media

Mohammad Reza Rasaei*, Fahime Firoozpour

Institute of Petroleum Engineering, School of Chemical Engineering, College of Engineering, University of Tehran, Tehran, Iran

Received: 19 January 2019, Revised: 11 March 2019, Accepted: 23 April 2019

Abstract

Simulating fluid flow at the micro level is an ongoing problem. Simplified macroscopic flow models like Darcy's law is unable to estimate the fluid dynamic properties of porous media. The digital sample reconstruction by high-resolution X-ray computed tomography scanning and fluid-dynamics simulation, together with the increasing power of super-computers, allow to carry out pore-scale simulations through digitally-reconstructed porous samples. The pore-scale flows which derived from computational fluid dynamics are then evaluated using the finite volume method implemented in the open-source platform OpenFOAM®. In this work, to verify the solver in porous media, we simulated fluid flow around a sphere in body-centered cubic (bcc) lattice and calculated the dimensionless permeability for a wide range of radius and porosity; the results are comparable with those obtained by using Carman-kozeny equation. Then this solver is performed on a realistic sample to investigate the effect of sample size on calculated permeability and tortuosity and the mesh refinement levels for a fixed image resolution.

Keywords:
CFD,
Computed Micro-tomography,
Digital Rock Physics,
Finite Volume Method,
OpenFOAM,
Permeability

Introduction

"Permeability" is one of the key tools that characterize petroleum reservoirs and their potential. The permeability of a porous medium is simply its ability to allow fluids to flow through it. Permeability, like other physical properties of porous materials, is a function of the complex microstructure; investigation the correlation between the microstructural geometry and the large-scale properties of porous media is a challenging topic in a wide range of subjects such as petrology, hydrology, filtration, catalysis and the like.

The development of X-ray computed tomography (CT) has made it feasible to provide images in three dimensions with a resolution of microns [1,2], which is adequate to capture the void geometry of many reservoir rocks.

At the pore scale, the single-phase flow in porous media is governed by the Stokes equation [3]. At the macro-scale, the fluid flow is commonly described by Darcy's law [4] and

* Corresponding author
E-mail: mrasaei@ut.ac.ir (M.R. Rasaei)

characterized by the macroscopic permeability, which can be evaluated by integrating the local fields.

A lot of different studies on fluid flow have been conducted for several decades. However, Pore-scale simulations of porous media by direct simulations of the local equations in a micro-tomographic image are relatively novel [5]. Different numerical methods have been investigated to understand flow characterizations. Mostaghimi et al. [6], using a finite-difference solver to simulate flow through digital samples of rock cores at the scale of pores at low Reynolds-number. Boomsma et al. [7] carried out numerical simulations of laminar flow through a cluster of two unit cells, each consisting of eight idealized pores of an open cell metal foam. In this study, a finite-volume method (FVM) is used to solve the incompressible, steady Navier-Stokes equations through the real porous media using structured hexahedral meshes. Gerbaux et al. [8] reconstruct digital samples of three open-cell metallic foams from X-ray tomography. Various unstructured, tetrahedral or cubic meshes are constructed. The microscopic Stokes flow through the foams is solved by FVM algorithms and one D3Q19 Lattice Boltzmann Method. The numerically computed and experimentally measured hydraulic permeabilities are in good agreement with each other and with available literature data.

Numerically, several aspects can influence the computed macroscopic permeability such as the numerical method. Finite volume [9,10] and lattice Boltzmann [11,12] are the two most commonly used methods for pore-scale flow characterization. However, we cannot neglect the difference between permeability which calculated by these two methods [13,14]. Besides, considering a continuous approach such as the FV method, the mesh refinement affects also the local flow simulation and consequently macroscopic properties calculations.

Materials and Methods

Fluid Flow Equations in Porous Media

To calculate effective parameters such as permeability, it is essential to compute the velocity field within the void space of the medium. The velocity profile of the fluid flowing through the pore space can be obtained by solving the base equations of fluid mechanics, the Navier-Stokes equations. We solve the local governing equations for incompressible fluid flow which are conservations of mass and momentum, respectively:

$$\nabla \cdot v = 0 \tag{1}$$

$$\frac{\partial \rho v}{\partial t} + \nabla \cdot (\rho v v) = -\nabla P + \rho g + \mu \nabla^2 v \tag{2}$$

where ρ is density, **v** = (u, v, w) is velocity vector, P is pressure, and μ is the viscosity. Fluid flow in petroleum reservoirs is often categorized in laminar flow range and the advective inertial forces in Navier-Stokes equations are small compared with viscous forces and can be ignored (Bear 1988) [15]. Thus, the governing equations reduce to stokes equation:

$$\nabla \cdot v = 0 \tag{3}$$

$$\mu \nabla^2 v = \nabla P \tag{4}$$

Numerical Methods to Solve Navier-Stokes Equations

The numerical simulations were performed in this research using the open-source OpenFOAM-5.0 CFD software package [16], which is based on the finite volume approach for the discretization of the governing equations. To solve the pressure-velocity coupling, most of the

fluid dynamics software is based on the Semi-Implicit Method for Pressure-Linked Equations (SIMPLE) algorithm [17] for steady-state.

Validation

To numerically verify the accuracy and efficiency of the simpleFoam solver of the OpenFOAM, we simulate three-dimensional creeping flow through an array of equal-sized spheres in bcc structure by this solver. Then we compared our results to the Carman-kozeny equation:

$$\frac{k}{d_p^2} = \frac{1}{180}\frac{\phi^3}{(1-\phi)^2} \tag{5}$$

Simulations were performed on a lattice with dimensions of 256 256 256 units with sphere radii differ from 10 to 110. Periodic boundary condition was imposed to front-back and top-bottom faces, the no-flow condition was imposed exactly at grain boundaries and constant pressure condition was imposed to outlet face. For inlet face, we conducted two different series boundary condition: constant velocity and constant pressure.

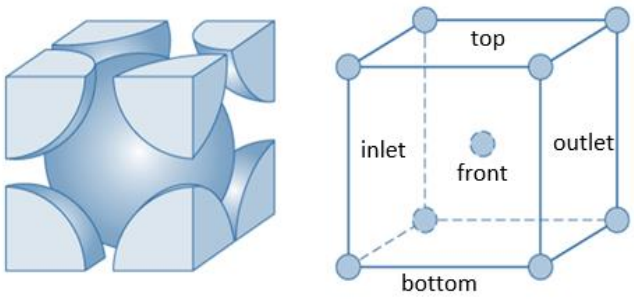

Fig. 1. Scheme of body-centered cubic lattice.

Fig. 1 shows a scheme of body-centered cubic lattice. Dimensionless permeability versus porosity curve of the lattice structure for the different radius is depicted in Fig. 2. Simulation data were compared against the Carman-kozeny equation; results were in good agreement. Fig. 2 illustrates that different boundary condition has no significant influence on outputs. Pressure field, velocity field and streamlines result of simulation for the sphere with radius 60 are presented in Figs. 3-6.

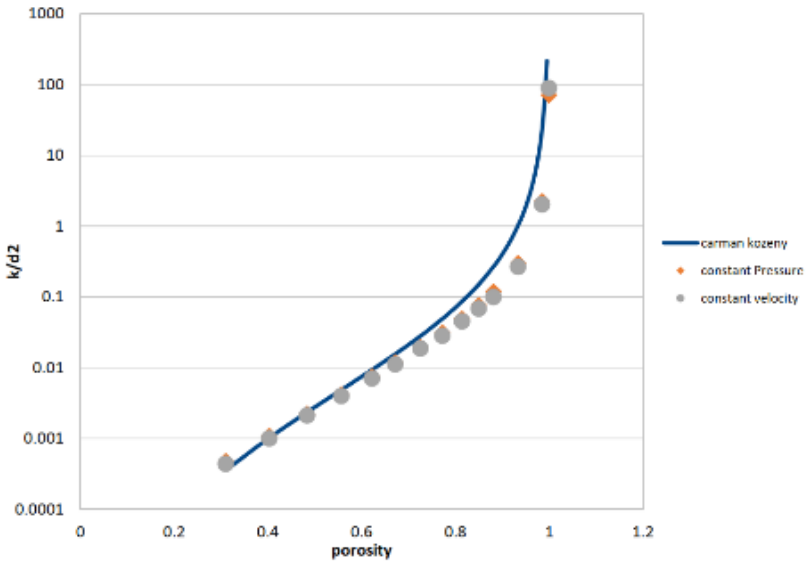

Fig. 2. Dimensionless permeability versus porosity of a bcc lattice

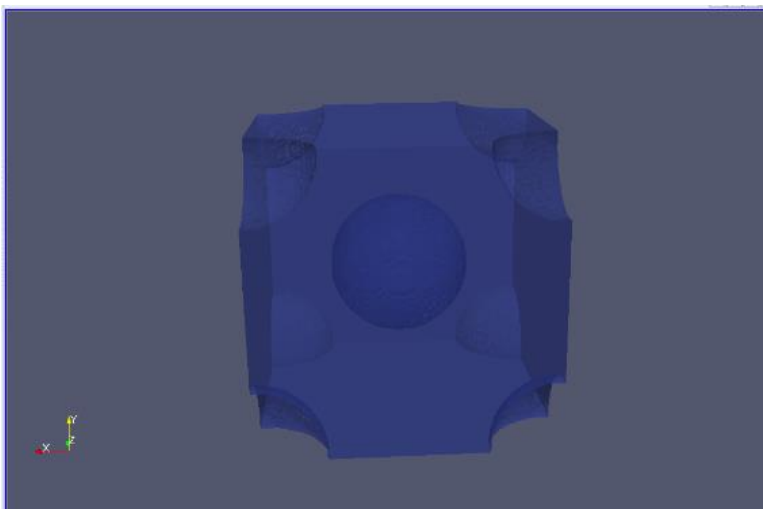

Fig. 3. Void space around sphere

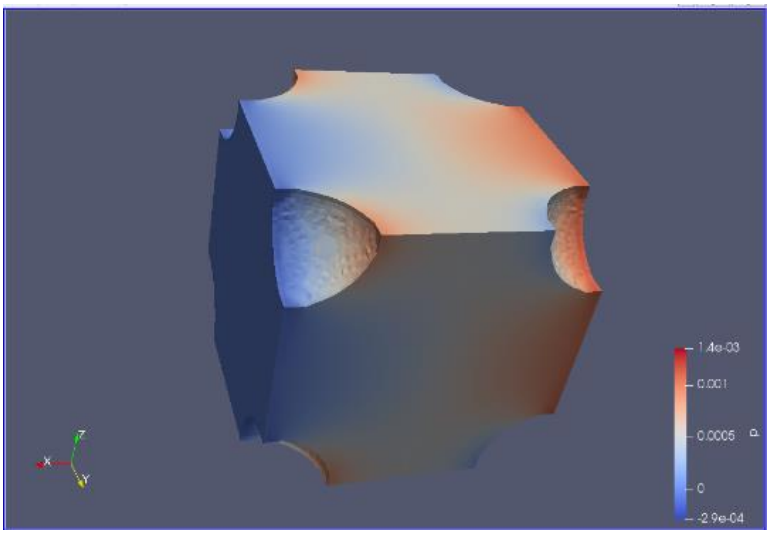

Fig. 4. Pressure field in void space for single phase

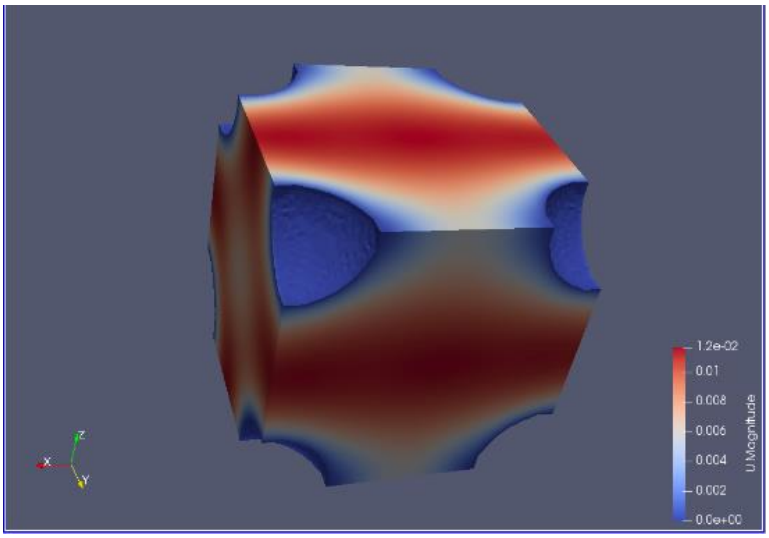

Fig. 5. Velocity magnitude in void space

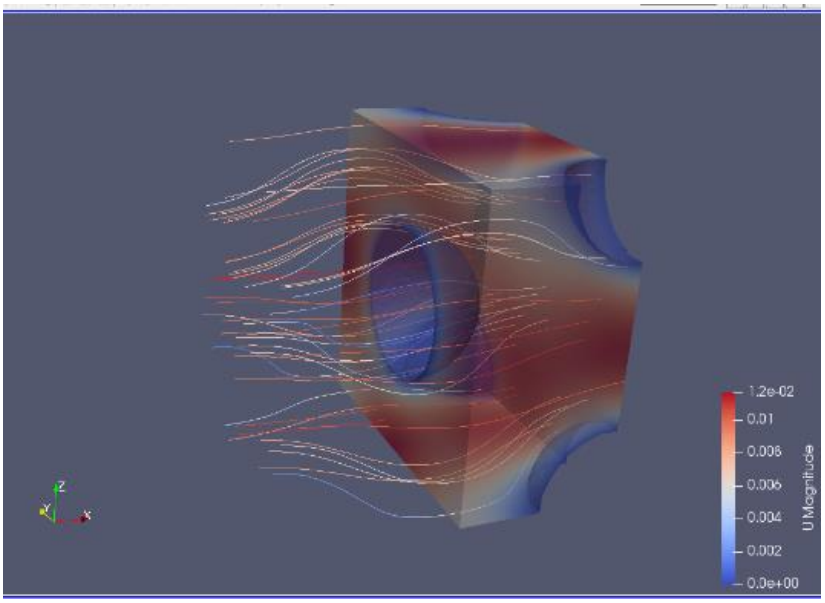

Fig. 6. Streamlines around spheres in void space

Results and Discussion

We now present the results from flow simulation on a real porous media obtained from micro-CT imaging of a core plug. In this work, a sandstone sample is used. The voxel size is 8.683 μm and the size of the considered digital sample, shown in Fig. 7, is 300^3 voxels. The porosity is 14.1%. The experimental absolute permeability of the rock from which the small plug was extracted is about 1.97 Darcy. Pressure distribution, velocity field, and streamlines of single-phase flow are shown below. In Fig. 8 the pressure drop is showed from inlet to outlet. Fig. 9 illustrates that velocity magnitude proportion to throat radius. In Fig. 10 the streamlines were started from the high-pressure part continues to the low-pressure part.

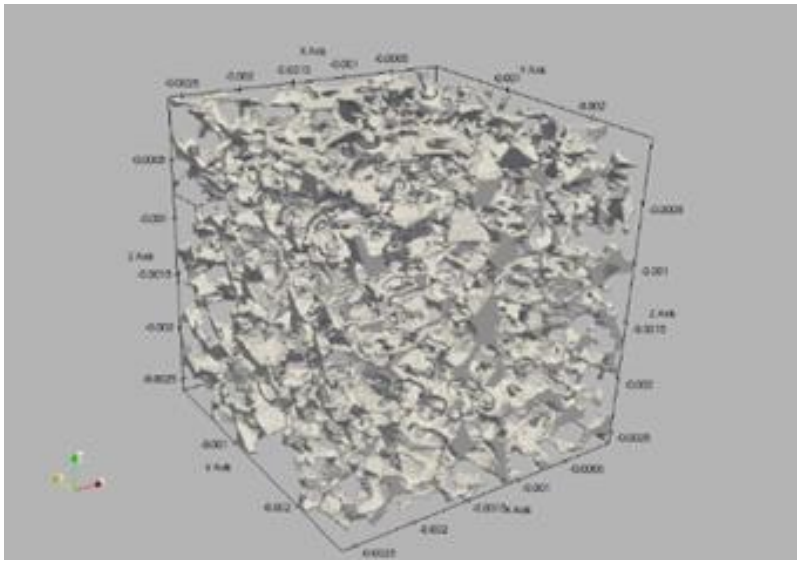

Fig. 7. Pore space of a sample 300×300×300

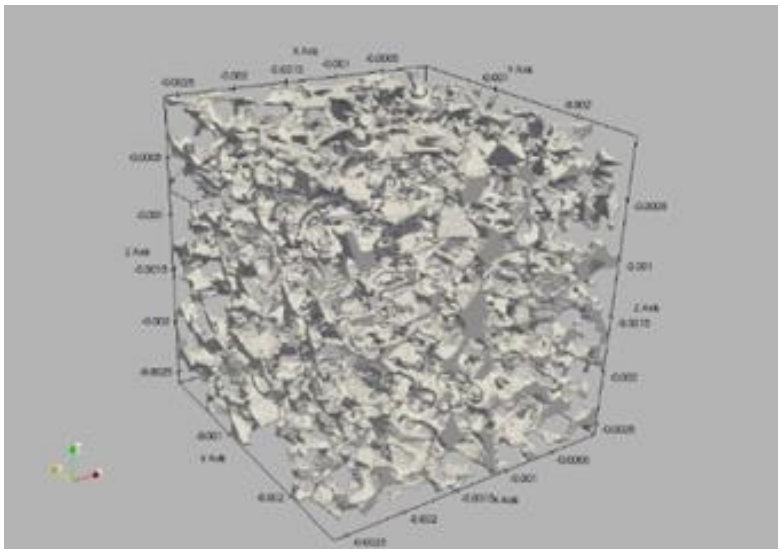

Fig. 8. Pressure distribution of single-phase flow

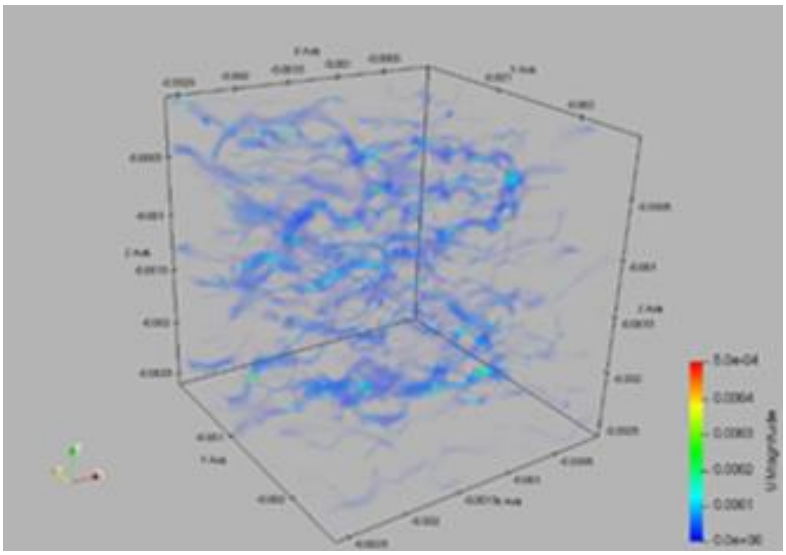

Fig. 9. Velocity field of single-phase flow

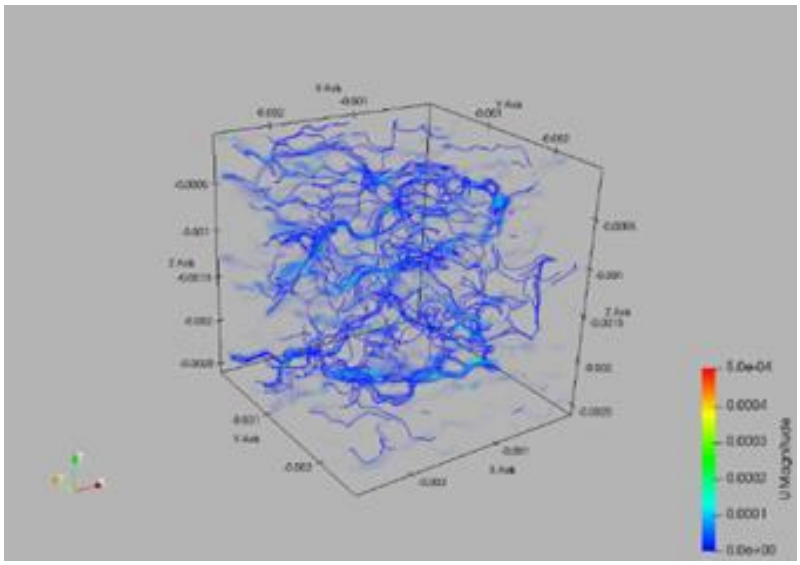

Fig. 10. Velocity field of single-phase flow

Permeability Prediction

The flow of a single-phase fluid is simulated for a sandstone sample of 300×300×300 pixels for different directions. Similar simulations have been performed for smaller sections of the primary sample.

The subsamples are selected according to the pattern shown in the Fig. 11. The permeabilities calculated from the results of these simulations are presented in Table 1. It can be seen that the sample size examined has significant effects on the results of flow simulation. It can be concluded that the sample size has significant effects on the results of flow simulation, therefore, finding a representative size is a challenging task.

Table 1. Porosity and directional permeability of samples

Size of sample	Direction of pressure gradient (i)	k_{xi}(darcy)	k_{yi}(darcy)	k_{zi}(darcy)	Effective porosity
100×100×100	X	2.7231736	0.6596557	0.1201848	0.14284901
100×100×100	Y	0.25705193	2.7586484	0.3096149	0.14284896
100×100×100	Z	0.0312942	0.336982635	1.295253312	0.14284901
150×150×150	X	2.743253952	0.1806742	0.013665816	0.12959755
150×150×150	Y	0.240650356	2.66658263	0.012730702	0.12959752
150×150×150	Z	0.150125395	0.083645277	1.680516441	0.12959752
200×200×200	X	2.898268518	0.047080775	0.272853845	0.13687854
200×200×200	Y	0.152894353	2.690117367	0.104070587	0.13687854
200×200×200	Z	0.124510666	0.033883736	1.513291197	0.13687854
250×250×250	X	2.9756319	0.22059233	0.32574771	0.13603194
250×250×250	Y	0.39047575	3.1099309	0.1247839	0.13603194
250×250×250	Z	0.1298363	0.1140137	1.82652691	0.13603194
300×300×300	X	2.7886349	0.01095066	0.41591417	0.134596904
300×300×300	Y	0.18219765	2.4296902	0.03999209	0.134596904
300×300×300	Z	0.1606448	0.0576169	1.94462126	0.134596904

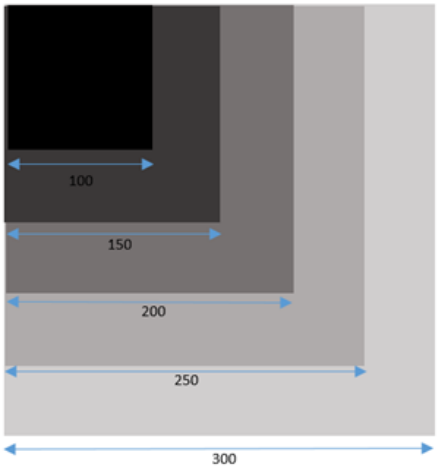

Fig. 11. Schematic of selected subsections

According to Darcy's law, we can calculate permeability from the applied pressure gradient ΔP, the viscosity of single-phase flow and the length of the system in the main direction of flow over which pressure gradient has been imposed:

$$k_{ij} = -\frac{\mu}{\Delta P_j V_{bulk}} \int v_i \, dv \text{ for i,j = x,y,z} \quad (6)$$

Where v_i is the i-th component of the velocity vector inside the sample.

One of the sources of difference between the results of numerical simulations and laboratory methods is the difference in the size of the examined sample in these two methods. Since computer hardware limits prevent flow simulations on large enough samples.

We also conducted another set of simulation to show the effect of mesh refinement on simulation outputs. Previous simulations have the same mesh number equal to their number of pixels. 5 mesh refinement levels used to investigate this issue on sample 150×150×150 pixels. the results of flow simulation in the x-direction are shown in Table 2.

Table 2. Mesh number and calculated permeability

Mesh refinement	k_x(darcy)
75×75×75	1.602542757
100×100×100	2.0161142
150×150×150	2.743253952
200×200×200	2.7923657
300×300×300	2.7953527

Table 2 shows that equal mesh number and pixel number have enough accuracy for this sample, in another word, the optimized mesh number is the same as pixel number.

Tortuosity Calculation

Tortuosity is one of the key parameters to study in porous media. Tortuosity is defined as the ratio of the length of the actual path of the fluid particles to the shortest path length in the direction of the flow:

$$\tau = \frac{l_{actual}}{l_{shortest}} \tag{7}$$

Tortuosity value is always greater than one. According to Sousa and Nabovati [18], the tortuosity can be calculated using the next equation:

$$\tau = \frac{\sum_{i,j,k} v_{mag}(i,j,k)}{\sum_{i,j,k} |\, v_x(i,j,k)|} \tag{8}$$

where the flow is in the x-direction.

Table 3. Calculated tortuosity for subsamples

Size of sample	Calculated tortuosity
100×100×100	1.080
150×150×150	1.083
200×200×200	1.102
250×250×250	1.083
300×300×300	1.095

The porous media sample was selected for the simulation was relatively heterogeneous. As it was shown in Table 3, the size of the subsection has an effect on calculated tortuosity.

Conclusions

We studied simpleFoam as an accurate solver of OpenFOAM to simulate Stokes flow at the pore scale in porous media directly on binarized pore-space images. It uses the Semi-Implicit

Method for Pressure-Linked Equations (SIMPLE) algorithm to solve steady-state flow for laminar and turbulent flow regimes. We used it to simulate incompressible single-phase flow through bcc lattice and porous media on micro-CT images to calculate permeability and tortuosity. The dimensionless permeability of the bcc lattices comparison was in a good agreement with the Carman-Kozeny equation. Since permeability is significantly affected by the size of investigated samples; finding representative elementary volume size of a sample rock has great importance. On the other hand, studying large samples face computer hardware limitations. We compared mesh refinement level outputs, the calculated permeability is affected by grid size and in this case, the optimum grid size is equal to the resolution size of the binary image.

Nomenclature

g	gravitational acceleration (m^2/s)
k	absolute permeability (darcy)
$l_{shortes}$	shortest path length (m)
P	pressure (pa)
t	time (s)

Greek letter

μ	viscosity (pa.s)
ν	velocity (m/s)
ρ	density ($kg/m^{3)}$
τ	tortuosity
φ	porosity

Reference

[1] Coenen J, Tchouparova E, Jing X. Measurement parameters and resolution aspects of micro X-ray tomography for advanced core analysis. InProceedings of the International Symposium of the Society of Core Analysts, UAE.(SCA 2004-36) 2004 Oct.

[2] Flannery BP, Deckman HW, Roberge WG, D'AMICO KL. Three-dimensional X-ray microtomography. Science. 1987 Sep 18;237(4821):1439-44.

[3] Bear J. Dynamics of fluids in porous media–American Elsevier pub. Comp., Inc. New York, 764p. 1972.

[4] Whitaker S. Flow in porous media I: A theoretical derivation of Darcy's law. Transport in Porous Media. 1986 Mar 1;1(1):3-25.

[5] Spanne P, Thovert JF, Jacquin CJ, Lindquist WB, Jones KW, Adler PM. Synchrotron computed microtomography of porous media: topology and transports. Physical Review Letters. 1994 Oct 3;73(14):2001.

[6] Mostaghimi P, Bijeljic B, Blunt M. Simulation of flow and dispersion on pore-space images. SPE Journal. 2012 Dec 1;17(04):1-31.

[7] Boomsma K, Poulikakos D, Ventikos Y. Simulations of flow through open cell metal foams using an idealized periodic cell structure. International Journal of Heat and Fluid Flow. 2003 Dec 1;24(6):825-34.

[8] Gerbaux O, Buyens F, Mourzenko VV, Memponteil A, Vabre A, Thovert JF, Adler PM. Transport properties of real metallic foams. Journal of Colloid and Interface Science. 2010 Feb 1;342(1):155-65.

[9] Lemaitre R, Adler PM. Fractal porous media IV: three-dimensional stokes flow through random media and regular fractals. Transport in Porous Media. 1990 Aug 1;5(4):325-40.

[10] Thovert JF, Adler PM. Grain reconstruction of porous media: Application to a Bentheim sandstone. Physical Review E. 2011 May 23;83(5):056116.

[11] Khan F, Enzmann F, Kersten M, Wiegmann A, Steiner K. 3D simulation of the permeability tensor in a soil aggregate on basis of nanotomographic imaging and LBE solver. Journal of Soils and Sediments. 2012 Jan 1;12(1):86-96.
[12] Pazdniakou A, Adler PM. Dynamic permeability of porous media by the lattice Boltzmann method. Advances in Water Resources. 2013 Dec 1;62:292-302.
[13] Manwart C, Aaltosalmi U, Koponen A, Hilfer R, Timonen J. Lattice-Boltzmann and finite-difference simulations for the permeability for three-dimensional porous media. Physical Review E. 2002 Jul 29;66(1):016702.
[14] Andrä H, Combaret N, Dvorkin J, Glatt E, Han J, Kabel M, Keehm Y, Krzikalla F, Lee M, Madonna C, Marsh M. Digital rock physics benchmarks—Part I: Imaging and segmentation. Computers & Geosciences. 2013 Jan 1;50:25-32.
[15] Bear J. Dynamics of Fluids in Porous Media. Courier Corporation; 1988.
[16] OpenFOAM: The Open Source CFD Toolbox User Guide
[17] Patankar S. Numerical heat transfer and fluid flow. CRC press; 1980 Jan 1.
[18] Nabovati A, Sousa AC. Fluid flow simulation in random porous media at pore level using lattice Boltzmann method. InNew Trends in Fluid Mechanics Research 2007 (pp. 518-521). Springer, Berlin, Heidelberg.